FEBS 30031 FEBS Letters 579 (2005) 6037–6043

Cloning, expression, characterisation and three-dimensional structure determination of *Caenorhabditis elegans* spermidine synthase

Veronica T. Dufe[a], Kai Lüersen[b], Marie-Luise Eschbach[b], Nashya Haider[b], Tobias Karlberg[a], Rolf D. Walter[b,*], Salam Al-Karadaghi[a,*]

[a] *Department of Molecular Biophysics, Center for Chemistry and Chemical Engineering, Lund University, P.O. Box 124, 221 00 Lund, Sweden*
[b] *Department of Biochemistry, Bernhard Nocht Institute for Tropical Medicine, Bernhard-Nocht-Str. 74, D-20359 Hamburg, Germany*

Received 26 July 2005; revised 14 September 2005; accepted 16 September 2005

Available online 5 October 2005

Edited by Irmgard Sinning

Abstract The polyamine synthesis enzyme spermidine synthase (SPDS) has been cloned from the model nematode *Caenorhabditis elegans*. Biochemical characterisation of the recombinantly expressed protein revealed a high degree of similarity to other eukaryotic SPDS with the exception of a low affinity towards the substrate decarboxylated *S*-adenosylmethionine (K_m = 110 μM) and a less pronounced feedback inhibition by the second reaction product 5′-methylthioadenosine (IC_{50} = 430 μM). The *C. elegans* protein that carries a nematode-specific insertion of 27 amino acids close to its N-terminus was crystallized, leading to the first X-ray structure of a dimeric eukaryotic SPDS.

Keywords: Nematodes; Polyamine synthesis; Inhibitors

1. Introduction

The ubiquitously distributed polyamines spermidine and spermine are aliphatic polycations that are involved in numerous cellular functions. Changes of intracellular polyamine concentrations were shown to correlate with growth and differentiation processes of pro- and eukaryotes. In polyamine synthesis, spermidine synthase (SPDS, putrescine aminopropyltransferase) catalyses the transfer of an aminopropyl moiety of decarboxylated *S*-adenosylmethionine (dcAdoMet) to putrescine, resulting in the formation of spermidine and 5′-methylthioadenosine (MTA). The precursor molecules putrescine and dcAdoMet are provided by the two key enzymes of the pathway, ornithine decarboxylase (ODC) and *S*-adenosylmethionine decarboxylase (AdoMetDC). Some eukaryotes possess a second aminopropyltransferase, spermine synthase (spermidine aminopropyltransferase), and consequently contain spermine [1–3].

SPDS have been characterised from many sources [1,2] and only recently, the first crystal structure of an aminopropyltransferase has been solved. The SPDS of the prokaryote *Thermotoga maritima* was analysed in ligand-free state as well as complexed with the substrate-product analogue *S*-adenosyl-1,8-diamino-3-thiooctane (AdoDATO) [4]. In contrast to the dimeric SPDS of eukaryotes, the *T. maritima* enzyme was found to have a tetrameric organisation. A monomer of *T. maritima* SPDS can be subdivided into an N-terminal and a C-terminal domain, the latter exhibiting similarity to the topology found in numerous nucleotide and dinucleotide-binding enzymes and in *S*-adenosylmethionine-dependent methyltransferases. The binding site of AdoDATO is formed by amino acid residues that are well conserved among the known SPDS. Hence, a universal catalytic mechanism for SPDS was suggested. This was further confirmed by the X-ray structure of the human SPDS, solved by one of the structure genomics consortia (PDB code 1ZDZ).

The polyamine synthesis pathway of the free-living nematode *Caenorhabditis elegans* encompasses the enzymes ODC, AdoMetDC and SPDS [5–8], whereas a homologous spermine synthase gene is lacking. The three enzymes exhibit a tissue-specific expression pattern in *C. elegans* suggesting that the intestine represents the main place of polyamine production [7]. *C. elegans* is a well established model organism to study general biological processes like for example development. Consistent with reports on other organisms [3,9], growth of *C. elegans* depends on polyamines, since ODC null mutants that do not have access to exogenous polyamines exhibit a stage-specific block of embryogenesis [10].

Here, we report on the molecular cloning, recombinant expression and biochemical characterisation of *C. elegans* SPDS. Analysis of the crystal structure confirmed a homodimeric organisation of the nematode enzyme and revealed a high degree of conservation of the overall fold when compared with the structure of the homotetrameric *T. maritima* SPDS. Furthermore, a nematode-specific insertion that has been identified close to the N-terminus of the *C. elegans* and other nematode SPDS was found to be located in close proximity to the substrate binding site.

2. Material and methods

2.1. Chemicals

Trans-4-methylcyclohexylamine (4-MCHA) and (*S*,*R*)-dcAdoMet were generous gifts from Keijiro Samejima (Josai University, Saitama, Japan). [1,4-^{14}C]Putrescine dihydrochloride (107 mCi/mmol) and [^{14}C] spermidine trihydrochloride (112 mCi/mmol) were from

*Corresponding authors. Fax: +49 40 42818 418 (R.D. Walter), +46 46 2224692 (S. Al-Karadaghi).
E-mail addresses: walter@bni-hamburg.de (R.D. Walter), salam.al-karadaghi@mbfys.lu.se (S. Al-Karadaghi).

Abbreviations: AdoDATO, *S*-adenosyl-1,8-diamino-3-thiooctane; AdoMetDC, *S*-adenosylmethinone decarboxylase; AdoMet, *S*-adenosylmethionine; dcAdoMet, decarboxylated *S*-adenosylmethionine; DTT, dithiothreitol; 4-MCHA, *trans*-4-methylcyclohexylamine; MTA, 5′-methylthioadenosine; ODC, ornithine decarboxylase; 3′-RACE, 3′-rapid amplification of cDNA ends; SPDS, spermidine synthase

0014-5793/$30.00
doi:10.1016/j.febslet.2005.09.050

Amersham-Biosciences (Freiburg, Germany). MTA and cyclohexylamine were purchased from Sigma Aldrich (München), spermidine and putrescine from Fluka AG (Neu-Ulm).

2.2. C. elegans *culture and nucleic acid preparation*

The *C. elegans* strain Bristol N2 was cultured under standard conditions at 22 °C in the presence of *E. coli* strain OP50. Worms were separated from bacteria by sucrose flotation [11]. Total RNA was extracted by homogenising worms in the presence of TRIZOL™ according to the manufacturer's instructions (Invitrogen).

2.3. *Cloning of* C. elegans *SPDS*

A putative *C. elegans* SPDS is annotated in the *C. elegans* genome on chromosome II (gene Y46G5.19, EMBL Accession No. AL110485). The corresponding open reading frame was amplified by PCR using *C. elegans* cDNA or a *C. elegans* λ-Zap cDNA library (Stratagene) as template and gene-specific oligonucleotides based on the identified genomic sequence CeSPDSExS: 5′-GGATCCCATGAACAAGCTGCACAAGGGA-3′ and CeSPDSExAS: 5′-AAGCTTCTACTCCAAAGCATTTTTGAC-3′ (introduced restriction sites for *Bam*HI and *Hin*dIII are underlined). PCR was performed as follows: 95 °C for 2 min, 50 °C for 1 min, and 68 °C for 2 min, for 30 cycles using Elongase amplification system (Invitrogen). The PCR product was subcloned for sequence analysis into pCRII™ vector using T/A cloning (Invitrogen). The nucleotide sequence was determined as described in Sambrook et al. [11]. The 3′ region of the SPDS mRNA was determined by using the rapid amplification of cDNA ends (RACE) Marathon kit (Clontech) with total *C. elegans* RNA as described by the manufacturer. PCR was performed using the obtained Marathon cDNA library of *C. elegans* as template and the gene-specific oligonucleotide CeSPDS-S1 5′-GAACGAGTTCGACGTAA-3′ (sense) and the oligo-dT-primer (antisense). The identified RACE products were cloned into pCRII™, sequenced and analysed.

The open reading frame of *C. elegans* SPDS was cloned into pTrcHisB vector (Invitrogen) to produce a His-tag fusion protein. The recombinant expression plasmid pTrcHisB:*Ce*SPDS was sequenced to ensure that the inserts were in the correct reading frame. Subsequently, the *E. coli* strain BLR (DE3) was transformed with pTrcHisB:*Ce*SPDS.

2.4. *Recombinant expression and purification of* C. elegans *SPDS*

A fresh overnight culture from a single colony of the *E. coli* expression cells containing pTrcHisB:*Ce*SPDS was diluted 1:100 in Luria–Bertani medium supplemented with 100 μg/ml ampicillin and grown at 37 °C until the OD_{600} reached 0.5. Expression was initiated with 1 mM isopropyl β-D-thiogalactoside. The cells were grown for additional 4 h at 37 °C before being harvested by centrifugation at $10000 \times g$ for 15 min at 4 °C. The cell pellet was resuspended in lysis buffer containing 0.1 mM phenylmethylsulfonyl fluoride, sonified and centrifuged at $100000 \times g$ for 1 h (TFT 55.38, Centricon T-1065, Kontron). Recombinant *C. elegans* SPDS was purified from the supernatant by chelating chromatography on Ni–NTA agarose (Qiagen) according to the manufacturer's recommendation. Protein was dialysed against 1000 volumes of buffer A (50 mM KH_2PO_4, pH 7.4, containing 1 mM EDTA, 0.1 mM dithiothreitol (DTT) and 0.1 mM phenylmethylsulfonyl fluoride).

To determine the molecular weight of the *C. elegans* SPDS, the eluate of the chelating chromatography was subjected to fast protein liquid chromatography on a calibrated Superdex S-200 column (2.6 cm × 60 cm) equilibrated with buffer A at a flow rate of 2 ml min^{-1}. Protein concentration was determined by the method of Bradford [12]. The homogeneity of the enzyme preparations were analysed by SDS–PAGE and subsequent Coomassie blue-staining [13].

2.5. *SPDS enzyme assay*

Aminopropyltransferase activity was determined by measuring the formation of radiolabelled reaction products from [^{14}C] putrescine or [^{14}C] spermidine following Samejima et al. [14]. Briefly, the reaction mixture in a final volume of 100 μl contained 50 mM potassium phosphate buffer, pH 7.0, 1.0 mM DTT, 1.0 mM EDTA, 200 μM of (*S*,*R*)-dcAdoMet, 200 μM putrescine (50 nCi [^{14}C] putrescine) or 200 μM spermidine (50 nCi [^{14}C] spermidine) and 200 ng recombinant *C. elegans* SPDS enzyme. Following 15 min of incubation at 37 °C, the reaction was terminated by heating for 5 min at 95 °C.

Separation of the reaction product was performed by thin layer chromatography on silica gel 60 sheets (Merck) with ethylenglycolmonomethylether, propionic acid and H_2O saturated with NaCl (140:30:30, v/v/v) as the mobile phase [15]. 10 μl of the assay together with 2 μl of each 50 mM polyamine standards were applied onto the sheets and run for 4 h. Spermidine and putrescine were visualised either by ninhydrin staining at 60 °C or by autoradiography (BIOMAX, Kodak). Spots were cut out and radioactivity was measured in a Packard-Tricarb 2000 liquid scintillation counter using 3 ml Packard UltimaGold? Liquid scintillation cocktail.

For the determination of K_m values, concentrations of putrescine varied from 25 to 750 μM and of *S*-dcAdoMet from 10 to 300 μM. The synthetic dcAdoMet preparation that was used contains the biologically active *S*-isomer together with the biologically inactive *R*-form of dcAdoMet in a 52–48 ratio. However, it has been demonstrated previously that *R*-dcAdoMet does not have any effect on SPDS enzyme reaction [16]. Kinetic parameters were calculated by Lineweaver–Burk plots using the program GRAPHPAD PRISM 1.02 (GraphPad Software, San Diego, CA). Inhibition tests were performed in standard assays supplemented with varying concentrations of the inhibitors cyclohexylamine (1–10 μM), 4-MCHA (0.5–50 μM) and MTA (10–1000 μM).

2.6. *Crystallization of* C. elegans *SPDS*

For crystallization, the recombinant *C. elegans* SPDS was purified as described above with minor modifications: Tris–HCl buffer, pH 8.0, was used instead of the phosphate buffer. Washes from the column were done with four bed volumes of 20–250 mM imidazole in wash buffer. Fractions were checked on SDS–PAGE and those containing the least impurities (100, 150 and 250 mM) were pooled and dialysed overnight against 20 mM Tris–HCl, pH 8.0, 1 mM DTT. The protein was concentrated to 5 mg/ml and the molecular weight checked on native PAGE.

Before setting up crystallization drops, the protein (5 mg/ml) was mixed with 100 μM of putrescine. Initial conditions were found using the Index Screen (Hampton Research) by mixing equal volumes of protein and well solutions in sitting drops at 21 °C. Platelet crystals appeared after one day in many conditions containing PEG 3350 and different salts. 25% PEG 3350, 0.2 M lithium sulphate, 0.1 M Tris–HCl buffer, pH 8.0 was chosen because the crystals looked better as the pH increased from 5.5 to 8.0. Most crystals grew together and were twinned. Further screening for better conditions with Additive Screen 3 (Hampton Research) was done. Addition of 0.01 M DDT gave fairly single crystals near the edges of the drop. The final crystallization condition consisted of 25% PEG 3350, 0.2 M lithium sulphate, 0.1 M Tris–HCl, pH 8.0, 0.01 M DTT well solution and 10 μl drop (4 μl protein-putrescine and 6 μl well solution) as increasing the drop size gave more single crystals. The crystals diffracted to 2.5 Å at the synchrotron and belonged to space group $P2_1$ with cell dimensions $a = 59.99$ Å, $b = 99.23$ Å, $c = 67.85$ Å, $\beta = 107.20$, with two molecules per asymmetric unit, and solvent content of 55%.

2.7. *Data collection and processing*

Diffraction data were collected at the beamline XO6SA of the Swiss Light Source, Paul Scherrer Institut, Villigen, Switzerland. Crystals were transferred to a drop containing a cryoprotectant consisting of 18 μl reservoir solution and 3 μl PEG 400 for a few seconds before flash freezing in liquid nitrogen stream at 100 K. Data were processed using the XDS package [17]. Data quality was checked with program TRUNCATE [18]. A summary of data statistics is shown in Table 1.

2.8. *Structure determination and refinement*

Initial phases were calculated by molecular replacement using the program Phaser [19] with anisotropic correction. Two molecules per asymmetric unit were searched for using chain C of the *T. maritima* SPDS structure (pdb Accession No. 1INL). Rigid body refinement of the solution was done with Refmac5 [20]. Model bias was removed using prime-switch in RESOLVE [21]. Successive rounds of model building, temperature factor refinement and positional refinement were done with programs O [22], CNS v 1.1 [23] and REFMAC5 [20], respectively. Non-crystallographic symmetry was used in the refinements.

Twenty water molecules were initially picked with Arp/wARP [24] and the rest were subsequently built using the program O. The model was checked with PROCHECK [25].

Table 1
Data collection and refinement statistics

Wavelength (Å)	0.89978
Cell parameters	
a (Å)	59.99
b (Å)	99.27
c (Å)	67.85
β (°)	107.2
Space group	$P2_1$
Resolution range	20.0–2.5
No. of observed/unique reflections	65 243/25 260
Completeness (%)	94.9(88.4)
$I/\sigma(I)$	9.97(2.38)
Rmrgd-F (%)	15.0 (56.6)
Molecules/asymmetric unit	2
% Solvent/VM ($Å^3$/Da)	55.0/2.8
Refinement resolution (Å)	20–2.5
Total no. of reflections	24 926
Reflections in working set	24 573
Reflections in test set	353
R-factor/R_{free} (%)	20.9/25.7
Wilson's B-factor ($Å^2$)	56.4
Overall B-factor ($Å^2$)	50.55
Water molecules	92
Bond length RMSD (Å)	0.016
Bond angles RMSD (°)	1.900
Ramachandran plot quality (%)	
Most favored	85.7
Additional allowed	13.9
Generously allowed	0.2
Disallowed	0.4

3. Results and discussion

3.1. Characterisation of C. elegans SPDS cDNA

A 945 bp PCR fragment was amplified from *C. elegans* cDNA using gene-specific oligonucleotides based on the EMBL genomic nucleotide sequence Accession No. AL110485. The cDNA sequence encodes an open reading frame that shows high similarity to amino acid sequences of known SPDS. However, the obtained nucleotide sequence does not resemble the cDNA sequence published in the Sanger Centre GenBank [Accession No. AL110485]. Here, an additional exon of 156 bp was proposed within intron IV. We could not confirm this result by our cDNA sequences obtained either by PCR on reversed transcribed mRNA nor by clones obtained from a λ-Zap cDNA library. A rapid amplification of cDNA 3′ ends was performed using a Marathon cDNA library of *C. elegans* as template. A 600 bp PCR product was found that encompasses the entire 3′ UTR of 56 bp including a typical polyadenylation signal sequence (AATAAA) located 20 bp upstream of the poly $(A)^+$ tail. Analyses of the 5′ UTR have been performed previously [6]. In conclusion, the *C. elegans* SPDS cDNA consists of 1013 bp and encodes a polypeptide of 314 amino acids with a deduced molecular mass of 35.0 kDa.

3.2. Characterisation of the recombinant C. elegans SPDS

C. elegans SPDS was recombinantly expressed as His-tag fusion proteins in *E. coli*. One litre of bacterial culture yielded about 10-mg purified protein. SDS–PAGE analysis revealed a single band with a molecular mass corresponding to 38 kDa including the His-tag of 3 kDa (Fig. 1). This is in good accordance with the predicted molecular mass of 35.0 kDa based on the amino acid sequence deduced from the cDNA.

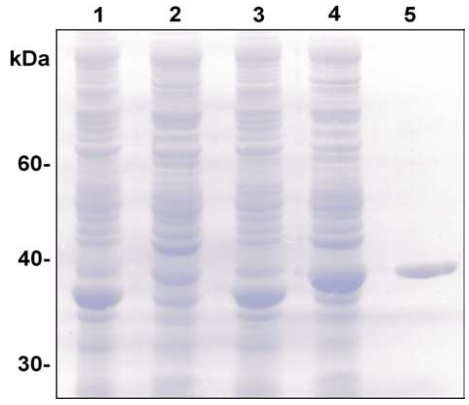

Fig. 1. SDS–PAGE analysis of the recombinant *C. elegans* SPDS. Lanes 1–5 represent protein extracts from *E. coli* BL21(DE3) induced with 1 mM IPTG (see Section 2). Coomassie blue-stained SDS–PAGE (10% polyacrylamide separation gel) of the $100\,000 \times g$ pellet (lane 1) and supernatant (lane 2) of lysed cells containing pTrcHisB without insert, of the $100\,000 \times g$ pellet (lane 3) and supernatant (lane 4) of lysed cells containing pTrcHisB:*Ce*SPDS and of recombinant His-tagged *C. elegans* SPDS purified by Ni–NTA-chelating chromatography (lane 5). The size of the protein standard is shown in kDa on the left.

The molecular mass of the *C. elegans* protein lies in the same range as those reported for the SPDS from mammals (35 kDa), *E. coli* (36.5 kDa) and plants like *N. sylvestris* (38.7 kDa) [16,26,27]. Performing gel filtration on a calibrated Superdex S-200 column resulted in a single peak corresponding to a molecular weight of 78 000 (data not shown), indicating a dimeric structure of the enzymatically active *C. elegans* SPDS. Most SPDS exhibit a homodimeric structure [1]. The *T. maritima* SPDS, however, forms a tetramer [4].

The recombinant *C. elegans* enzyme has a specific activity of 1.8 μmol min^{-1} mg^{-1} protein resulting in a k_{cat} of 69.2 min^{-1}. This is in the same range as those published for SPDS isolated from mammalian sources (660–1300 nmol min^{-1} mg^{-1}) [14,28]. The K_m value for putrescine was calculated to be 158 ± 27 μM (n = 5), which is comparable with the K_m values reported for mammalian enzymes (100 μM) [14,28]. Like for mammalian SPDS [29], the *C. elegans* enzyme is characterised by a high specificity towards putrescine. Hence, spermidine could not replace putrescine as aminopropyl acceptor (data not shown). The K_m value for the second substrate dcAdoMet was determined to be 111 ± 5 μM (n = 3), which is about 15-fold to 100-fold higher than those reported for mammalian SPDS [26,30]. A relatively high K_m value for dcAdoMet (35 μM) has also been reported for the *Plasmodium falciparum* SPDS [4]. The enzyme reaction of *C. elegans* SPDS is inhibited by the second product MTA with an IC_{50} of 430 μM (n = 2). Therefore, a physiological function of feedback inhibition by MTA seems to be unlikely in *C. elegans*. The mammalian SPDS is 10 times more sensitive towards MTA. A concentration of about 30 μM MTA is needed for 50% inhibition of enzyme activity [31].

C. elegans SPDS activity was affected by the synthetic inhibitors 4-MCHA and cyclohexylamine with IC_{50} values of 7.2 μM (n = 2) and 2.4 ± 0.7 μM (n = 4), respectively. This is in the same range as the IC_{50} values that have been reported for mammalian SPDS (8.1 μM for cyclohexylamine and 1.7 μM for 4-MCHA) [32,33]. Both compounds are known competitive inhibitors with respect to putrescine [1,33].

In conclusion, the *C. elegans* SPDS resembles the mammalian counterparts to a great extent. However, the low affinity for dcAdoMet and the feedback inhibitor MTA are specific for *C. elegans* SPDS.

3.3. Three-dimensional structure and dimeric organisation of C. elegans SPDS

The X-ray crystallographic structure of the *C. elegans* SPDS enzyme shows a homodimer (Fig. 2), which is in accordance with biochemical data presented above. Each subunit consists of two domains: A six-stranded β-sheet builds up the structural framework of the N-terminal domain (residues 3–92) and a Rossman-fold like unit builds up the C-terminal domain (residues 93–314). A total of 26 residues at the N-terminus (residues 1–2 and 18–40) and fourteen residues at the C-terminus (residues 190–202) could not be modelled due to weak electron density. Although the crystallisation was attempted in complex with one of the substrates, putrescine, no electron density for it was detected in the active site, which may suggest that the presence of both substrates is a prerequisite for their stable binding. This function could be regulated by the nematode-specific insertion, the possible structural role of which is discussed below.

Non-crystallographic symmetry restraints were imposed on the dimer during refinement, thus the two independent subunits are identical with the RMSD between the Cα atoms being 0.08 Å. Subunit interaction was analysed using the Protein–Protein Interactions Server (http://www.biochem.ucl.ac.uk/bsm/PP/server). The dimer interface is formed by packing interactions between residues from helices and strands (α1, α6, α7, α8, α9, β1, β2, β3, β11, β12, β13), and the loops between strands and helices (β2–β3, β3–β4, β6–α1, β11–α6, β12–β13, α7–α8, α8–α9), of each subunit. The interface buries around 1660 Å^2 of the total accessible surface area of each monomer. A total of 95 residues from both subunits, of which 64 are non-polar, contribute to surface interactions. There are thirteen hydrogen bonds and six bridging waters. Most of the hydrogen bonds are formed through main chain atoms. Two hydrogen bonds (one/subunit) involve the side chains of Y74 and Q49, and two hydrogen bonds involve the side chain of T73 and the main chain of P44.

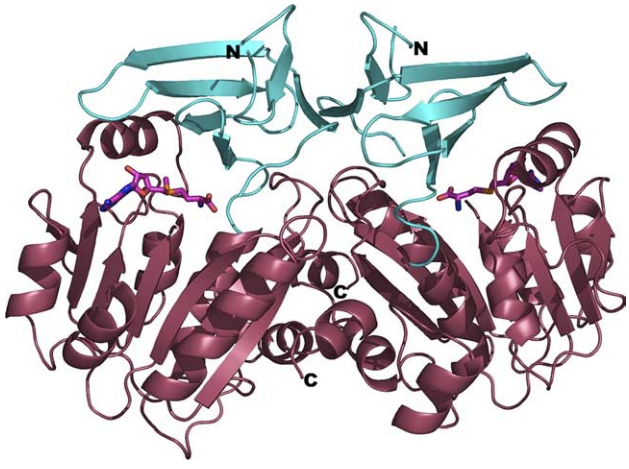

Fig. 2. A schematic view of the dimer of *C. elegans* SPDS. The N-terminal domain (residues 3–92) of each monomer is coloured in cyan and the C-terminal domain (residues 93–314) in brown. The AdoMet molecule modelled from the human SPDS is shown in sticks to mark the location of the active site. The positions of the N- and C-termini are marked. Figure was prepared using PYMOL [35], http://pymol.sourceforge.net/.

In contrast to the dimeric organisation of the *C. elegans* SPDS, the three-dimensional structure of *T. maritima* SPDS is a homotetramer, which is probably better described as a dimer of dimers. The subunits within each of the dimers are organised in a fashion which resembles domain organisation in *C. elegans* SPDS. The interface between the subunits within a dimer buries around 1894 Å^2 of the accessible surface area of each monomer, compared to 1660 Å^2 in *C. elegans* SPDS. There are 22 H-bonds at the interface compared to thirteen in CeSPDS. The *T. maritima* SPDS tetramer is stabilised by a tight β-barrel with a hydrophobic core formed by four N-terminal hairpins (built up by strands β1 and β2). The same hairpin is also present in *C. elegans* SPDS. However, a comparison of the amino acid sequences of *T. maritima* and *C. elegans* enzymes shows that this region is not well conserved, especially between bacterial and eukaryotic sequences (Fig. 3A). These differences may prevent the formation of the barrel structure by the *C. elegans* enzyme. There are also 12 additional residues at the N-terminus of *T. maritima* SPDS, when compared to the *C. elegans* enzyme. These residues contribute additional interactions between the subunits, which may enhance the stability of the tetramer. Probably one should also take into account the nematode-specific loop, which in the *C. elegans* SPDS structure is located between strands β1 and β2 (Figs. 3B and 4). This loop may also affect the stability of the hairpin formed by β1 and β2 and may interfere with the formation of a tetramer.

3.4. Comparison with other SPDS structures

Pairwise sequence alignment using BCM search launcher (http://searchlauncher.bcm.tmc.edu/) reveals that the amino acid sequence of *C. elegans* SPDS is very similar to the counterpart of the human-parasitic nematode *Brugia malayi* [unpublished] (55%) and also to other known SPDS with sequence identities of 57% to the human [27], 48% to the *Nicotiana sylvestris* [34], 41% to the *E. coli* [35] and 43% to the *T. maritima* [4] proteins (Fig. 3A).

The structure of *T. maritima* and human SPDS were determined in complex with the inhibitor AdoDATO and with AdoMet, respectively. The structures demonstrate a high level of conservation of the overall topology (Fig. 4). Thus, the structures of *T. maritima* and human SPDS could be superimposed on the *C. elegans* enzyme with rmsd (root-mean square deviation) for the Ca-atoms of around 1 Å. The largest differences between the *C. elegans* and *T. maritima* enzymes are found in the region of helices α3, α4 and α6 (residues 142–151, 168–177 and 230–242, respectively; *C. elegans* numbering). There are shifts in the Cα atom positions of up to 3 Å in this region. A superposition of the structures of human and *T. maritima* SPDS shows that the differences are maintained for helices α3 and α6, while helix α4 superimposes well on the corresponding helix from the *T. maritima* enzyme. Although the structure of a ligand-free human enzyme is not available, a comparison between the apo- and inhibitor complex structures of *T. maritima* SPDS does not show any differences in the position of this helix. Taking into account that α4 builds up part of the substrate binding cleft, the difference between the human and *C. elegans* enzymes may be of interest for future design of nematode-specific inhibitors.

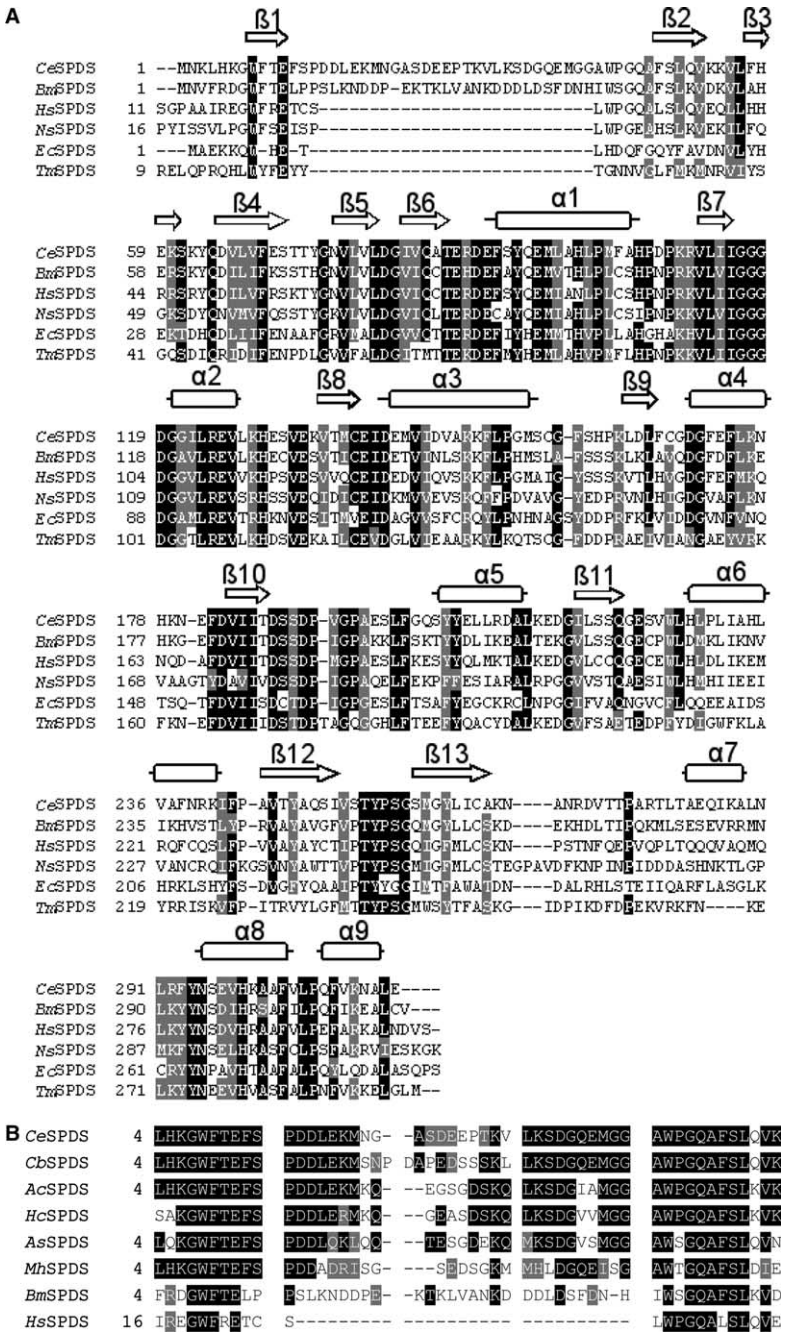

Fig. 3. Alignment of SPDS amino acid sequences (A). The amino acid sequence of *C. elegans* SPDS is compared with the *B. malayi*, the human [EMBL Accession No. AAA36633], the *N. sylvestris* [EMBL Accession No. BAA24535], the *E. coli* [EMBL Accession No. P09158] and the *T. maritima* SPDS. Amino acid residues that are invariant in at least four additional sequences are shaded in black, similar amino acids in grey. The N-terminus of the human, the *N. sylvestris* and the *T. maritima* sequence is omitted as indicated. Gaps (−) are introduced to provide maximum similarity. The position of the secondary structure elements is shown along the sequence. (B) The nematode-specific insertion of *C. elegans* SPDS is aligned with the respective regions of putative SPDS from the nematodes *C. briggsae* [www.genome.wustl.edu/gsc/Projects/C.briggsae/], *Ancylostoma caninum* [EMBL Accession No. AW626946], *Haemonchus contortus* [EMBL Accession No. BF060177], *Ascaris suum* [EMBL Accession No. BI783107] *Meloidogyne hapla* [EMBL Accession No. BM883048] and *B. malayi*. The N-terminus of the *H. contortus* sequence is unknown. The respective region of the human SPDS is aligned to indicate the insertion. Identical amino acid residues are shaded in black, similar in grey. Gaps (−) are introduced to provide maximum similarity.

The structure of *T. maritima* SPDS in complex with AdoDATO shows that the putrescine-binding site is a hydrophobic cavity, which includes two negatively charged sites responsible for anchoring the amino groups of the molecule. In particular, Asp170 (*T. maritima* numbering) has been proposed to be responsible for deprotonating the attacking amino group of putrescine, whereas Tyr76 and Ser171 are thought to be involved in binding and proper orientation of the diamine. The corresponding residues in the *C. elegans* enzyme are Tyr94, Asp188 and Ser189. In total, 20 amino acid residues are involved in interactions with the inhibitor. Of these 16 are conserved, whereas four have been exchanged in *C. elegans*

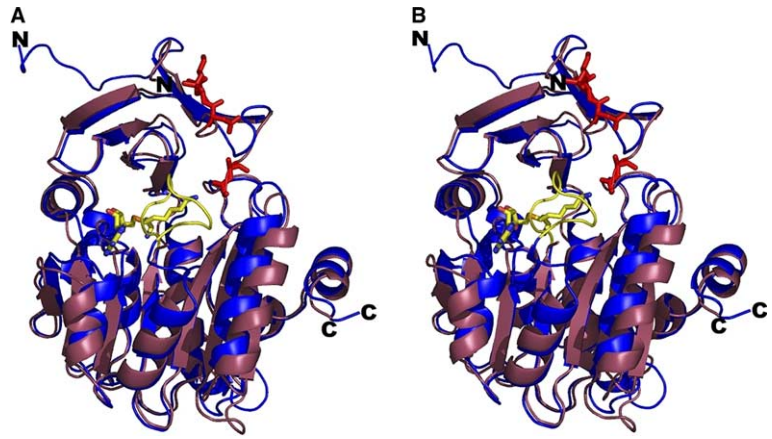

Fig. 4. A superposition of the structures of *T. maritima* (brown) and *C. elegans* SPDS. The gatekeeper loop in the *T. maritima* enzyme is shown in yellow. The few nematode-specific insert residues that could be modelled are shown in red sticks. The positions of the N- and C-termini in both proteins are marked.

(Met67 to Gln85, His77 to Gln95, Gln178 to Pro195 and Trp244 to Met261). Fig. 5 shows the overall topology of the substrate binding site of *C. elegans* SPDS. A superposition on the structure of the *T. maritima* enzyme (Fig. 5A) shows that the position and conformation of some side chain and main chain atoms (Tyr94, Asp170, Phe172, Tyr256, Gln221, and Met261) is different. Some of these differences are due to the shifts in the position of helices α4 and α6, as described above. It should also be noted that the superposition of the *T. maritima* apo- and inhibitor-bound structures shows no differences in side-chain conformations within the active site cleft. Thus, the observed differences between the *C. elegans* and *T. maritima* SPDS may not depend on the absence of bound substrate in the *C. elegans* enzyme. The active site clefts of the human and *C. elegans* SPDS is much more conserved, with only few differences in amino acid position (Fig. 5B).

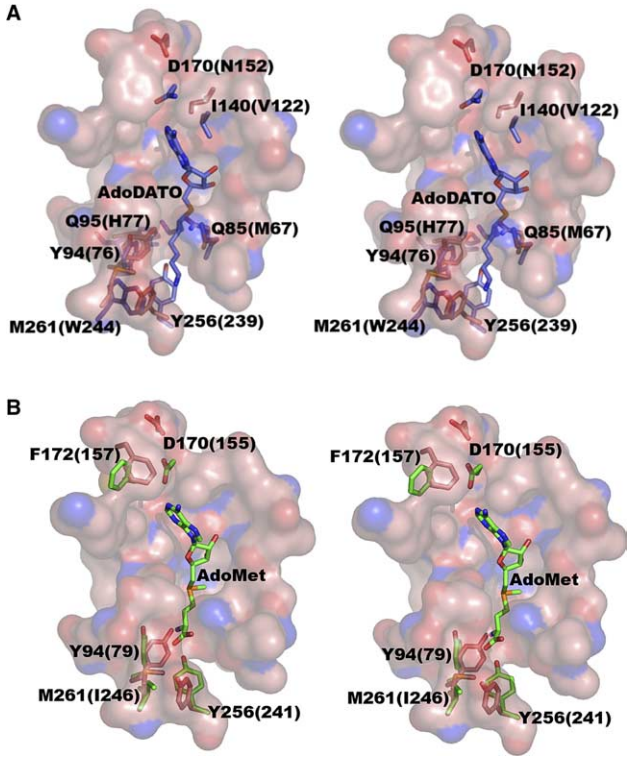

Fig. 5. Surface representation of the active site of SPDS. (A) A stereo view showing the active site of *C. elegans* SPDS. Side chains of residues that have different conformations in *T. maritima* (blue sticks) and *C. elegans* SPDS are shown. Also shown is the inhibitor AdoDATO in the position found in the complex with the *T. maritima* enzyme. The residue numbers/names in brackets are for *T. maritima* SPDS. (B) A stereo view showing the active site of *C. elegans* SPDS. Side chains of residue that have different conformations in human (green sticks) and *C. elegans* SPDS are shown. There is only one substitution; I246 of the human enzyme is M261 in *C. elegans*. Also shown is AdoMet in the position found in the complex with human SPDS. The residue numbers/names in brackets are for the human SPDS.

Another feature of the active site of SPDS is a loop region, described by Korolev et al. [4], who proposed it to function as a gatekeeper to or from the binding pocket of the *T. maritima* enzyme. In the three-dimensional structure this region is located between strand β10 and helix α5 (Figs. 3A and 4). Six of these amino acid residues are conserved in the nematode sequence 189-SSDPVGPAE-197. Moreover, an amino acid residue corresponding to Thr175 of the *T. maritima* loop is lacking in the *C. elegans* and all other SPDS. Unfortunately in the presented three-dimensional structure from *C. elegans* the region of the gatekeeper loop is disordered, most probably due to the lack of substrate in the active site. Also in the apo-structure of *T. maritima* SPDS this region is disordered.

The nematode-specific insertion mentioned above contains 27 amino acids and is located close to the N-terminus (Figs. 3B and 4). The amino acid sequence of the insertion reflects the phylogenetic relationship of the nematodes according to the taxonomic classification by Blaxter et al. [34]. *Caenorhabditis briggsae*, *Ancylostoma caninum*, *Ascaris suum* and *Haemonchus contortus* are members of the same clades as *C. elegans* and the identity of their SPDS insertions, with respect to the *C. elegans* sequence, is 74–62%. The value for *Meloidogyne hapla* is 30% and *B. malayi* with a value of 11% (3 identical amino acids in 27) exhibits the greatest phylogenetic distance to *C. elegans*. In the three-dimensional structure the region corresponding to the nematode-specific sequence is unfortunately disordered. However, it is clear that this loop, which represents a unique structural feature of nematode SPDS, is located in close proximity to the putative gatekeeper

loop (Fig. 4). This location may indicate an interaction between these two regions of the molecule in the regulation of the function of the enzyme. However, the contribution of this interaction has to be elucidated in further studies.

Another feature of *C. elegans* SPDS is a coiled region between Ala 278 and Thr282, which in the *T. maritima* structures is a short helix (Pro262–Phe267). Curiously, in the adjacent region a coil between Arg265 and Glu270 (*T. maritima* numbering) is substituted by a helix in *C. elegans*. This difference is specific for the *T. maritima* enzyme, since in the human SPDS the structure in this region is similar to that from *C. elegans*. The coordinates have been deposited in the Protein Data Bank with Accession No. 2B2C.

Acknowledgements: We thank the staff of the Swiss Light Source synchrotron for support. This work was supported by the Deutsche Forschungsgemeinschaft (Wa 395/10-4 and Wa 395/13) and the Vereinigung der Freunde des Tropeninstituts Hamburg (N.H.). S. Al-Karadaghi is supported by a grant from FLÄK (Forskarskolan i läkemedelsvetenskap). The authors are grateful to Prof. Keijiro Samejima for kindly providing dcAdoMet and 4-MCHA. A part of this work was conducted in partial fulfilment of the requirement for a PhD of N. Haider from the University of Hamburg.

References

[1] Tabor, C.W. and Tabor, H. (1984) Polyamines. Annu. Rev. Biochem. 53, 749–790.
[2] Pegg, A.E., Poulin, R. and Coward, J.K. (1995) Use of aminopropyltransferase inhibitors and of non-metabolizable analogs to study polyamine regulation and function. Int. J. Biochem. Cell Biol. 27, 425–442.
[3] Thomas, T. and Thomas, T.J. (2001) Polyamines in cell growth and cell death: molecular mechanisms and therapeutic applications. Cell Mol. Life Sci. 58, 244–258.
[4] Korolev, S., Ikeguchi, Y., Skarina, T., Beasley, S., Arrowsmith, C., Edwards, A., Joachimiak, A., Pegg, A.E. and Savchenko, A. (2002) The crystal structure of spermidine synthase with a multisubstrate adduct inhibitor. Nat. Struct. Biol. 9, 27–31.
[5] Macrae, M., Plasterk, R.H. and Coffino, P. (1995) The ornithine decarboxylase gene of *Caenorhabditis elegans*: cloning, mapping and mutagenesis. Genetics 140, 517–525.
[6] Da'dara, A.A. and Walter, R.D. (1998) Molecular and biochemical characterization of *S*-adenosylmethionine decarboxylase from the free-living nematode *Caenorhabditis elegans*. Biochem. J. 336, 545–550.
[7] Lüersen, K., Eschbach, M.L., Liebau, E. and Walter, R.D. (2004) Functional GATA- and initiator-like elements exhibit a similar arrangement in the promoters of *Caenorhabditis elegans* polyamine synthesis enzymes. Biol. Chem. 385, 711–721.
[8] Heby, O. (1981) Role of polyamines in the control of cell proliferation and differentiation. Differentiation 19, 1–20.
[9] Macrae, M., Kramer, D.L. and Coffino, P. (1998) Developmental effect of polyamine depletion in *Caenorhabditis elegans*. Biochem. J. 333, 309–315.
[10] Sulston, J. and Hodgkin, J. (1988) Methods in: The Nematode Caenorhabditis elegans (Wood, W.B., Ed.), pp. 587–606, Cold Spring Harbor Laboratory Press, Cold Spring Harbor, NY.
[11] Sambrook, J., Fritsch, E.F. and Maniatis, T. (1989) Molecular Cloning: a Laboratory Manual, 2nd edn, Cold Spring Harbor Press, Cold Spring Harbor, NY.
[12] Bradford, M.M. (1976) A rapid and sensitive method for the quantitation of microgram quantities of protein utilizing the principle of protein–dye binding. Anal. Biochem. 72, 248–254.
[13] Samejima, K., Raina, A., Yamanoha, B. and Eloranta, T. (1983) Purification of putrescine aminopropyltransferase (spermidine synthase) from eukaryotic tissues. Methods Enzymol. 94, 270–276.
[14] Haider, N., Eschbach, M.L., de Souza Dias, S., Gilberger, T.W., Walter, R.D. and Lüersen, K. (2005) The spermidine synthase of the malaria parasite *Plasmodium falciparum*: molecular and biochemical characterization of the polyamine synthesis enzyme. Mol. Biochem. Parasitol. 142, 224–236.
[15] Dejima, H., Kobayashi, M., Takasaki, H., Takeda, N., Shirahata, A. and Samejima, K. (2003) Synthetic decarboxylated *S*-adenosyl-L-methionine as a substrate for aminopropyl transferases. Biol. Pharm. Bull. 26, 1005–1008.
[16] Kabsch, W.J. (1993) Automatic processing of rotation diffraction data from crystals of initially unknown symmetry and cell constants. J. Appl. Crystallogr. 26, 795–800.
[17] French, G.S. and Wilson, K.S. (1978) On the treatment of negative intensity observations. Acta Crystallogr., 517–525.
[18] Storoni, L.C., McCoy, A.J. and Read, R.J. (2004) Likelihood-enhanced fast rotation functions. Acta Crystallogr. D: Biol. Crystallogr. 60, 432–438.
[19] Murshudov, G.N., Vagin, A.A. and Dodson, E.J. (1997) Refinement of macromolecular structures by the maximum-likelihood method. Acta Crystallogr. D: Biol. Crystallogr. 53, 240–255.
[20] Terwilliger, T.C. (2000) Maximum likelihood density modification. Acta Crystallogr. D: Biol. Crystallogr. 56, 965–972.
[21] Jones, T.A., Zou, J.Y., Cowan, S.W. and Kjeldgaard, M. (1991) Improved methods for building protein models in electron density maps and the location of errors in these models. Acta Crystallogr. A 47, 110–119.
[22] Brunger, A.T., Adams, P.D., Clore, G.M., DeLano, W.L., Gros, P., Grosse-Kunstleve, R.W., Jiang, J.S., Kuszewski, J., Nilges, M., Pannu, N.S., Read, R.J., Rice, L.M., Simonson, T. and Warren, G.L. (1998) Crystallography & NMR system: a new software suite for macromolecular structure determination. Acta Crystallogr. D: Biol.Crystallogr 54, 905–921.
[23] Perrakis, A., Morris, R. and Lamzin, V.S. (1999) Automated protein model building combined with iterative structure refinement. Nat. Struct. Biol. 6, 458–463.
[24] Laskowski, R.A., MacArthur, M.W., Moss, D.S. and Thorton, J.M. (1993) PROCHECK: a program to check the sterochemical quality of protein structures. J. Appl. Crystallogr. 26, 283–291.
[25] Hashimoto, T., Tamaki, K., Suzuki, K. and Yamada, Y. (1998) Molecular cloning of plant spermidine synthases. Plant Cell Physiol. 39, 73–79.
[26] Samejima, K. and Yamanoha, B. (1982) Purification of spermidine synthase from rat ventral prostate by affinity chromatography on immobilized *S*-adenosyl(5′)-3-thiopropylamine. Arch. Biochem. Biophys. 216, 213–222.
[27] Kajander, E.O., Kauppinen, L.I., Pajula, R.L., Karkola, K. and Eloranta, T.O. (1989) Purification and partial characterization of human polyamine synthases. Biochem. J. 259, 879–886.
[28] Pegg, A.E., Shuttleworth, K. and Hibasami, H. (1981) Specificity of mammalian spermidine synthase and spermine synthase. Biochem. J. 197, 315–320.
[29] Hibasami, H., Borchardt, R.T., Chen, S.Y., Coward, J.K. and Pegg, A.E. (1980) Studies of inhibition of rat spermidine synthase and spermine synthase. Biochem. J. 187, 419–428.
[30] Shirahata, A., Morohohi, T., Fukai, M., Akatsu, S. and Samejima, K. (1991) Putrescine or spermidine binding site of aminopropyltransferases and competitive inhibitors. Biochem. Pharmacol. 41, 205–212.
[31] Shirahata, A., Takahashi, N., Beppu, T., Hosoda, H. and Samejima, K. (1993) Effects of inhibitors of spermidine synthase and spermine synthase on polyamine synthesis in rat tissues. Biochem. Pharmacol. 45, 1897–1903.
[32] Wahlfors, J., Alhonen, L., Kauppinen, L., Hyvonen, T., Janne, J. and Eloranta, T.O. (1990) Human spermidine synthase: cloning and primary structure. DNA Cell Biol. 9, 103–110.
[33] Tabor, C.W., Tabor, H. and Xie, Q.W. (1986) Spermidine synthase of *Escherichia coli*: localization of the *speE* gene. Proc. Natl. Acad. Sci. USA 83, 6040–6044.
[34] Blaxter, M.L., De, L.P., Garey, J.R., Liu, L.X., Scheldeman, P., Vierstraete, A., Vanfleteren, J.R., Mackey, L.Y., Dorris, M., Frisse, L.M., Vida, J.T. and Thomas, W.K. (1998) A molecular evolutionary framework for the phylum Nematoda. Nature 392, 71–75.
[35] Delano, W.L. (2002) The PYMOL Molecular Graphics System, DeLano Scientific, San Carlos, CA, USA.